Smart Energy Management Algorithm for Load Smoothing and Peak Shaving Using Load Forecasting in Island Power Systems: A Healthcare-Critical Infrastructure Resilience Approach

Dr. Amina El-Sayed[1]*
Dr. Lukas Weber[2]
Prof. Sofia Marinova[3]
[1] University of Cape Town, Department of Biomedical Engineering and Health Energy Systems, Cape Town, South Africa
[2] University of Helsinki, Department of Health Informatics and Smart Energy Systems Engineering, Helsinki, Finland
[3] Medical University of Vienna, Institute of Clinical Infrastructure and Sustainable Energy Engineering, Vienna, Austria

Abstract:

In this study, a novel algorithm for the management of the power flows of an islanded power system was developed, capable of simultaneously achieving steadier conventional unit operation and shaving the demand peak values, for the days of the year that present a night peak in their load curve. The under investigation system is composed of Diesel Generators, a PV farm and a Battery Energy Storage System (BESS) with the power system's consumption to be relatively higher than its RES production. The proposed algorithm combines the use of a load forecasting methodology, a pattern recognition procedure and a custom optimal power flow scheduling algorithm. The prediction module was based on a feedforward artificial neural network, capable of short-term day ahead load forecasting. The forecasted day ahead load profile was then used as an input to the developed pattern recognition algorithm, in order to be classified based on its load curve shape (pattern). Subsequently, in case that the classification resulted in a clear night peak pattern, it was possible to estimate an hourly based trajectory for the diesel generators operation and derive the BESS charging setpoints, which result in the desired peak shaving and smoothing level simultaneously. In this way, it is possible to replace or substitute the highest power demand with stored renewable energy and to operate the diesel engines as steady as possible, diminishing the ramp up and the steep gradients before the night hours' peak. The algorithm was integrated in the overall system model in APROS software, where dynamic simulations were performed. The simulation results proved that by applying the proposed algorithm, a combined effect of smoother diesel generator operation and peak shaving with renewable energy is achievable even with the absence of PV overproduction, diminishing the variability of the load to be covered from the conventional units. Such an operation aims at enabling diesel engines to be rated at a lower, than currently, maximum capacity while increasing the share of the renewable energy penetration into the grid.

Keywords:

Battery Energy Storage System; Energy Management System; Load Forecast; Peak Shaving; Renewable Energy; Island Power Systems

1. Introduction

Nowadays, fundamental concepts related with energy production and consumption are continuously evolving and being reformed to meet the continuously emerging requirements imposed by the development of electrification strategies, based on the advantages offered by smart energy networks. Due to strict environmental regulations and limitations, energy utilities are forced to implement technical changes and alter their policy, in order to achieve a more sustainable and mainly renewable based operation [1]. This task may be feasible for large scale, highly interconnected grids.

On the contrary, for smaller and islanded grids, where renewable production presents a significant proportion of the total system production and with any excess of energy not to be easily exported, this goal is more difficult to be achieved. This task may be challenging even for electric power systems that present a relatively higher consumption compared to the RES production, yet enough to enhance the variability of the net load (i.e. demand load minus RES generation) curve (the low valley during the daylight time period). This issue has also been identified from the California Independent System Operator and reported as the “duck shape” problem [2]. This problem which is related to the time shifted maximization of the PV production compared to the night hour’s peak demand, is continuously deteriorating the smoothing level of the net load and exacerbates the ramp up requirements. This is a common issue for power systems that are still highly dependent on conventional power generation and the renewable share is now beginning to increase – as is the case for many islanded power systems which rely on diesel generators. In this perspective and especially for islanded systems, the robust grid operation is highly dependent on precise forecasts and the use of storage solutions, since the production/consumption power flows are required to be exclusively balanced on a local level. Currently, this is primarily addressed with the appropriate use of diesel generators. Abrupt changes in load conditions and sudden impulses of renewable energy injections into the grid are usually counterbalanced by promptly commissioning diesel generators for peak hour demand, forcing them to experience cold start-ups or to operate in variable power setpoints which result in fuel-consuming ramp-ups and ramp-downs. Both of these operational conditions are strongly related to high operating costs and reduced diesel engine lifetime, which in turn have a negative effect on grid operators and is also reflected into a high cost of electricity production. In addition, as stated in [3], commercial and industrial customers are subject to monthly maximum demand charges, which can be as high as 30% of the total electricity bills; thus peak shaving can be an efficient way to reduce those charges and relieve diesel generators from cost-intensive and energy-demanding ramps-up, when accelerating from base to peak load conditions.

Concerning the aforementioned inherent difficulties in operating islanded grids and with the aim of managing the power flows between production and consumption, battery energy storage systems (BESS) are considered as a promising option for smoothening net load curve fluctuations and enabling higher renewable power penetration simultaneously. Such a system can be inter-connected to the energy grid, providing ancillary services with frequency control or load smoothing by peak shaving during the hours of the day with high demand (i.e. midday hours), using stored energy from day periods with a relatively low demand (i.e. night hours). However, the most suitable operation strategy of the BESS, which is supervised by a centralized Energy Management System (EMS), is related to the shape of the load profile of the system and the type (in terms of stochasticity) of renewable power generation. Thus, for an islanded power system, where the load profile presents a high peak during late night hours and high photovoltaic (PV) generation during daylight hours, peak shaving with BESS energy stored from PV generation seems a rational approach. Specifically, this is the case for most South European islands, where the load profile is shaped mainly from activities related to tourism at night hours rather than energy devouring industries that operate during the daylight hours.

Considering the smart grids concept, a smart control and management system is necessary in order to achieve the most efficient and optimized BESS operation. Thanks to recent developments in time-series forecasting methodologies and the possibility to access a big amount of data related to the power system operation, an EMS can support a predictive strategy based on consumption/production forecasts and an objective function minimization. Therefore, load forecasting is a necessary stepping stone, in order to achieve better energy dispatch planning, which is of great significance for the steadier operation of conventional generators. A load forecasting can be implemented through various models, with artificial neural networks (ANNs) being one possible, relatively simple but accurate enough load forecasting methodology, to be integrated in smart EMS algorithms.

Aim of this study is the demonstration of the developed smart framework for the management and control of a BESS, through dynamic simulation. This framework combines load forecasting with pattern recognition, and a custom scheduling algorithm for the coverage of the island’s peak values

with renewable PV power, despite the lack of renewable energy overproduction. The function of the developed scheduling algorithm is not limited to the peak shaving time period, but also predefines a constant load operation of the conventional units during the off-peak hours. The combined effect of the peak shaving and load smoothing enables the diminishment of the "duck" shape evolution of the net load curve [2] and the higher renewable penetration at the same time. In Section 2, an extensive literature review of currently (state-of-the-art) developed predictive EMS algorithms is presented. In Section 3, the load forecasting process followed in this study is described, in Section 4 the novel scheduling algorithm, the clustering procedure and the system modelling are presented, while the results of the dynamic simulations are discussed in Section 5.

2. Literature review on data driven forecasting for predictive Energy Management Algorithms

Many studies related with short term load forecasting for power grids implementing numerous methodologies and algorithms from the field of time-series forecasting have been published so far. Among them, many versions of ANNs have proved to be a common approach [4,5]. In order to evaluate the performance of forecasting methodologies and their capability to forecast accurately, several statistical indicators are used such as Mean Squared Error (MSE), Mean Absolute Error (MAE) and Mean Absolute Percentage Error (MAPE) with the last being the most common for comparison actions [6]. In [7] a combined synergy of two ANNs, i.e. one for basic day ahead load forecasting and one for peak and valley forecasting was proposed, highlighting the strong correlation of temperature with load. The decent forecasting capability of shallow neural networks was also reported in [8], while the authors implemented a day ahead hybrid load forecasting using a divide-and-conquer hierarchical approach. The whole dataset was partitioned into smaller ones and each one was used to train a different ANN model. The Fuzzy C-means method was then used for clustering the load data points and Principal Component Analysis (PCA) for selecting the most suitable input features for each network. The combined result was considered as the final prediction. In this way, they reported the achievement of lower MAPE than that of classic ANNs or Bagged NNs. In [9] the hourly load curve of Spanish power system was modelled as a linear function of low and high frequency components considering a Long-Term Demand Model (LTDM), based on macroeconomic parameters for low frequency components, and calendar, temperatures and daylight effects for high frequency components. The model was used to forecast long-term annual peak and trough demand values and showed an overall improvement in MAPE compared with a nonlinear autoregressive exogenous (NARX) model which was used for validation. However, as the authors stated, the models in literature that present the highest accuracy in forecasting hourly electricity loads, with Neural Networks being among them, have a short prediction horizon (e.g. 24 h). This prediction horizon is considered adequate for the purpose of this study, therefore a higher complexity forecasting model is not necessary. Moreover, in [10] an ensemble of ANN networks was proposed and implemented for simultaneous load forecasting of many substations and it was shown that the results were significantly enhanced compared to the single ANN approach. In [11] a Least Squares Support Vector Machine was introduced for short term load forecasting that improved the results compared to benchmark methods. In [12] a novel multimodal Fuzzy-ARTMAP network was proposed for its faster convergence capability compared to backpropagation networks. Despite the tremendous developments in recent forecasting algorithms leading to higher accuracy forecasting results, the well-established, robust, with proven results, neural network methodology, was adopted in this study. The ANN model of this study was developed for the purpose of integrating a relatively simple but accurate enough prediction module to the overall developed power scheduling algorithm, described in a next section.

Predictive Energy Management Systems (EMS) are based on high quality forecasting models of both electricity demand and renewable energy production, which are simultaneously solved as an optimization problem, dealing both with operational setpoints and cost minimization. In the residential sector, such systems have been included into the operational platform of small-scale BESS, as in [13], where forecast-based algorithms with dynamic PV power feed-in limitations (in order to

avoid curtailment) were reformulated into linear optimization problems before being used for the identification of the optimum power use in a house. In this way, many operating strategies of battery charging and discharging could be accomplished, leading to increased self-sufficiency and less curtailed PV energy. In [14], a reactive power management algorithm was implemented to account for load forecasting uncertainties by introducing a range of values for the State of Charge (SoC) with a bounded trajectory of around 5% of the planned value, which was calculated to achieve electricity cost minimization along with both an associated increased battery lifetime and a simultaneous grid relief compensation. Another study [15] was focused on load forecasting aiming at increasing the battery lifetime of a PV when interconnected in the main MV/LV grid of a residential network, whereas in [16] a Kalman load model was developed for load forecasting based on past load values, temperatures and number of occupants in the house. In [17], a MPC was implemented for a PV and battery residential system with load forecasting based on ANNs and in [18] a FLC (Fuzzy Logic Controller) was used for active power control which resulted in load profile smoothening, while the proposed fuzzy EMS compensated for forecast errors. Nevertheless, all the above case studies were dealing with systems integrating enough renewable power, so that the charging process of the BESS was possible when the excess power condition (renewable power production > consumption) was occurring.

However, implementing such predictive energy management systems for large isolated power systems and BESS for grid scale applications can be more challenging, due to inherent difficulties related with the lack of grid supply as a backup alternative. In [19] it was stated that the operational strategy of the microgrid needs to adapt to the daily load pattern and therefore load forecasting is necessary to be integrated in the scheduling procedure. Nevertheless, in many proposed Energy Management Strategies, the load profile is considered either already known or it is measured online and consequently the optimization procedure becomes challenging. Additionally, the amount of renewable (PV) power generation in most studies – and in contrast to the present study - is considered large enough so as to be higher than the consumption at certain time periods. In studies such as [20], load forecasting was used for predicting the operation of a system with a high PV penetration and a BESS. Implementation of a parallel-series Complex Value NN and of a splined-based load forecasting showed better results compared to a trivial persistence predictor. Thus, it was possible to obtain reliable load forecasts that could be used for an optimized BESS operation scheduling (peak shaving or load smoothing). However, the forecasting methodology developed in their study was not integrated with the management system of the BESS. In [21] and [22] a simple linear regression model for load forecasting has been implemented in order to achieve optimal operation of a grid-scaled BESS for the power network of Hawaii island, considering also the large number of installed PV capacity on rooftops at the level of the distribution grid. Although the simulations showed that load peak shaving and dampening of load fluctuations were achieved, the BESS model was not detailed enough to include all the dynamic characteristics of charging/discharging processes while the BESS would be preferably charged from excess renewable power. In [23] a very similar peak shaving and load smoothing algorithm with additional voltage regulation capability was proposed. Nevertheless, the load forecasting was based on a linear regression model mostly incapable of capturing the nonlinear load variations, while a more complex optimization methodology (compared to the current study) was required for the BESS setpoint generation. In [24], a predictive real-time BESS control based on load forecasting with ANNs was implemented to provide both peak shaving and primary frequency control for the Germany power system at the same time. The MAPE achieved with the ANN in their study (1.87%), is slightly worse compared to the MAPE achieved in this study despite the fewer input variables of the present study's network. In [25] an integrated utility scale BESS was combined with the dispatchable feeder concept for a university campus consisting of dispatchable buildings loads with considerable PV generation. The dispatch planning was formulated as a trajectory tracking problem, which was solved using MPC for real-time feedback control of the BESS dispatch power, while at the same time compensating for day ahead load forecast errors, as in the present study. Load forecasting was implemented using a vector-autoregression technique based on similar days and by incorporating a NWM (Numerical Weather Model), while the authors

highlighted the possibility for a better performing forecasting tool to be plugged in their control structure (possibly an ANN forecasting module as it was employed in this study). The relation of forecast-based strategies with dispatch planning was also remarked in [26], examining the impact of forecast accuracy on the operational cost of an isolated microgrid, the operation setpoints of which were derived through a predictive optimization model. Synthetic load forecasts of different quality were produced and used in their simulations, in the absence of real time series data and an integrated load forecasting capability, which were then used by a rolling-horizon relatively complex optimization methodology for the next day power scheduling. Predictive energy management systems for a microgrid consisting of grid-tied BESS with PV generation were also examined in [27] and [28], where load and PV generation forecasts were provided as an input (known a priori) and were used in combination with an optimization problem for minimizing renewable curtailment power or grid consumption and consequently the electricity cost. However, the ability for power exchange with the main power grid interconnection presented an operating advantage over isolated microgrids. A cascaded central long-term EMS down to a short-term balancing EMS were simulated in [29]. In this case, load consumption was considered already known and day ahead scheduling was obtained, while at the same time supercapacitors were used by a local EMS for primary frequency control.

In [30] a hierarchical control scheme (tertiary, secondary) was proposed for a small-sized islanded microgrid but the load forecasts were considered already known and the PV power was exceeding consumption at certain times. In [31], the islanded microgrid management controller was based on a rule-based management strategy and did not have an integrated load prediction capability. In [32], an advanced MPC controller and an EMS strategy for a grid-connected or islanded grid was proposed, but the BESS could be charged only at the times of renewable overproduction. In addition, the load was predicted based on the power balance equations of the electrical grid model, which may be considerably different from the real system. In [33], a similar study as in [32] was characterized by the same lack of forecasting capability of the EMS. In [34], the control of the BESS in the microgrid under study relied on the surplus renewable energy and a PI control, whereas no load forecasting was integrated to their strategy. In [35], the developed PV BESS peak shaving algorithm was based on the power balance and a rule-based strategy, lacking a prediction of the load for the optimization of the battery trajectory. In [36], a highly complex optimization algorithm was introduced for the implementation of the developed energy management strategy based on local load measurements, but no forecasting was integrated to their method as they also pointed out that it is to be integrated in the future. Thus, the complexity of the online optimization in order to catch up with the load changes should require a highly intense computational effort.

Progress beyond the state-of-the-art

From the above review analysis, it is evident that the performance of islands' energy management system with BESS is highly correlated with a) the optimization targets, b) any operational constraints, c) the specific characteristics of the load profile, and d) the amount and type of installed renewable power. In the present study, the system under investigation refers to a small South-European island and is composed of Diesel Generators, a PV farm and a Battery Energy Storage System (BESS). The obtained real-world load data presented highly peak in the late hours which clearly dictates that a peak shaving overall approach is necessary. In addition, the fact that renewable electricity originates/comes from PV, the power generation of which can be easily and accurately forecasted, implies that a smart methodology can be developed.

In this manner, an algorithm for the management of the power flows was developed, capable of simultaneously achieving steadier conventional unit operation and shaving the demand peak values, for the days of the year that present a night peak in their load curve. Initially, a load forecasting method predict next day's load and PV production. The forecasted day ahead load profile is then used as an input to the developed pattern recognition algorithm, in order to be classified based on its load curve shape (pattern). Subsequently, in case that the classification indicated a clear night peak pattern, it is possible to estimate an hourly based trajectory for the diesel generators operation and derive the

BESS charging setpoints, which can lead to the desired peak shaving and smoothing level simultaneously.

The new aspect of the present study lies in the combination of the different algorithms in an overall methodology, able to predict, recognize and act accordingly. Benefits from the present work include:

- Integration of forecasting and clustering capabilities in the energy management system.
- The proposed BESS stores only renewable energy (PV production).
- The developed scheduling algorithm does not require a PV generation that exceeds the demand in order to charge the BESS. It creates the appropriate amount of "artificial" surplus of renewable energy to cover the energy amount to be shaved.
- Along with the shaving using stored renewable energy during the peak hours, the algorithm defines a single/specific level of operation for the conventional units. This results in an additional effect, the smoothing effect at the load curve during the off-peak hours.

These benefits were validated in the APROS simulation environment, where the scheduling algorithm was implemented as a custom signal-based EMS. In these simulations, the algorithm's daily forecast-based schedule dealt with the actual day's load and production values in order to obtain valid results.

3. Load Forecasting with Artificial Neural Network

3.1 Network structure and associated data

A forecasting model is a necessary subsystem that needs to be implemented in a predictive energy management algorithm, to enable the latter to incorporate future events. In this study, such a model was developed for future consumption values forecasting by implementing a simple single-hidden layer feedforward neural network. This neural network structure was chosen based on the well-known Kolmogorov theorem [37]. According to this, a single layer of hidden neurons with the appropriate number of perceptrons is considered to be sufficient for any function fitting problem, which is the case in this study. In this way, short-term load forecasting was mathematically formulated as a function fitting problem in which the hourly load time-series of a whole year were estimated. Specifically, the developed model was trained from past years load data (i.e. years 2014, 2015) provided from the South-European island's grid operator and the outputs were the load data for the next year (i.e. year 2016). A strong correlation between the trend of the load curve and the temperature data of the island was observed, rendering the latter an appropriate input for the developed neural network model. The hourly temperature data was produced by the long validated CFSR [38] numerical weather model (NWM) from representative grid points near the most densely inhabited areas of the island for the years examined, in order for the correlation of weather phenomena with electricity consumption to be intensified.

The inputs of the feedforward neural network were determined, based on common input variables for similar networks referred in load forecasting studies [3-7] and after a trial-and-error iterative procedure. Therefore, they were found to give the best results in terms of the MAPE, defined as:

$$MAPE = \frac{1}{N}\sum_{i=1}^{N}\left|\frac{Forecasted\ Load_i - True\ Load_i}{True\ Load_i}\right| \qquad \textit{Equation 1}$$

, where N is the data point number (*8760*). These inputs were i) the 48 values of the hourly consumption data of the two previous days, ii) the 24 values of previous day temperature data, iii) 7 binary values corresponding to the day of the week and iv) a binary variable which was used as an index for weekend days and working days. The network output consisted of a 24-variable vector containing the next day's forecasted load values. The structure of the developed networks is schematically depicted in Figure 1.

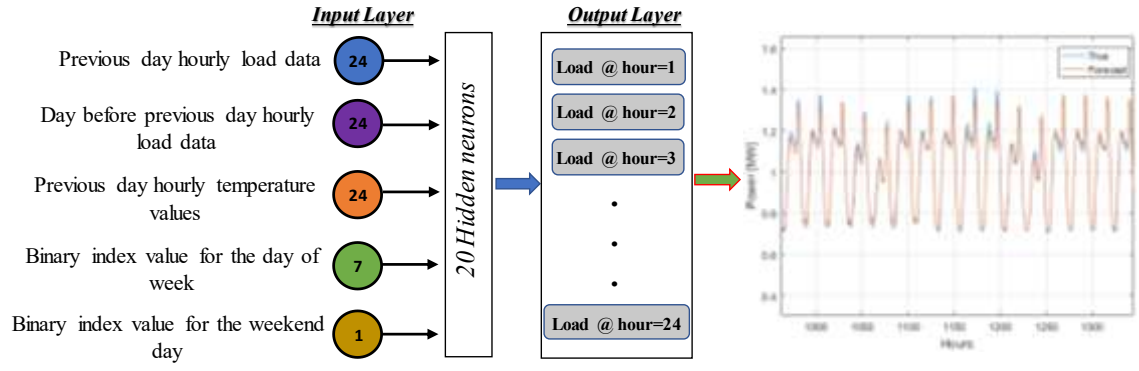

Figure 1: Developed Neural Network for load forecasting

The input variables, before the training procedure, were scaled in the interval [0, 1] so that every input had the same weighting despite the different physical scales, with which is related. For the same reasons, the binary values were chosen to be 0 or 1. For the training procedure, as it was stated above, data from years 2014 and 2015 were used in a backpropagation algorithm based on the Levenberg-Marquardt error minimization algorithm. This is basically a variation of the Newton's method using a scalar relaxation coefficient μ, which in the beginning of the training has a relatively high value and after each iteration is decreases into smaller values and eventually turns the procedure from a Gradient Descend into a Newton's method, which is faster and more efficient near the minimum error region. In this way, after each iteration the neuron's weight matrix and biases vectors are updated based on the following equation

$$\vec{x}_{k+1} = \vec{x}_k - [J^T J + \mu I] J^T \vec{e} \quad \text{Equation 2}$$

, where J is the Jacobian matrix of the network's errors $\vec{e}$. The latter are calculated based on the difference of the networks output $\vec{y}$ from target values $\vec{t}$. In order to generate the output y_j, the input argument u_j is transformed through a transfer function $f(u)$, which for this case study was selected to be the logistic sigmoid activation function, that is suitable for forecasting and curve fitting problems [4, 5, 8].

$$f(u) = \frac{1}{1 + e^{-\mathrm{u}}} \quad \text{Equation 3}$$

For n input signals x_k, the activation function argument u_j is calculated for the j neuron by using n input nodes as

$$u_j = \sum_{k=1}^{n} W_{jk} x_k - b_j \quad \text{Equation 4}$$

Each neuron output can be calculated as the weighted sum of the neuron's inputs, which are also outputs from a previous network layer, after being filtered from the activation function. The network's output vector from each layer is calculated based on Equation 5:

$$y_j = f\left(\sum_{k=1}^{n} W_{jk} x_k - b_j\right) \quad \text{Equation 5}$$

, where n is the number of the input signals, W_{jk} is the weight which corresponds to the strength of the connection channel (synapse) connecting input k to neuron j, and b_j is the applied bias. The mean squared error function (MSE) was used as a termination criterion for the training procedure and is calculated as (Equation 6):

$$MSE = \frac{1}{P}\sum_{p=1}^{P}(\vec{t}_p - \vec{y}_p)^T \cdot (\vec{t}_p - \vec{y}_p) = \frac{1}{P}\sum_{p=1}^{P}\sum_{m=1}^{M} e_{p,m}^2 \quad \text{Equation 6}$$

In the equation above, P is the number of training data batches used and p is the corresponding index for each training pattern applied. A single data batch is composed of the same number of elements as the number of input variables (80). The error vector $\vec{e}_p$ for each batch contains m elements, which are calculated as the differences between the target and network output m-dimensional vectors. The evaluation of the network output with respect to the target values was implemented with the correlation coefficient R as shown in Figure 2. The MSE parameter was first calculated for the validation data set, chosen to be around 4% of the training set, and then the overall network's performance was evaluated for the test set which was not ever used in the training process.

3.2 Network Results

After the network configuration procedure was completed and the best results were achieved, the linear regression of the targets relative to the outputs was calculated based on the correlation coefficient. This was calculated to be R=0.99189, which is considered as an acceptable value. In particular, from the scatter plot in Figure 2 it is possible to observe that the majority of the data points of the whole dataset (training, validation, test) are concentrated around the neighborhood of the perfect forecast line. The perfect forecast line is the straight line with an inclination of 45 degrees and represent the equality of the network's output with the actual value. Thereinafter, the outputs were scaled back to their physical scales, the overall network's performance was re-evaluated for the test set and a *MAPE=1.715%* was achieved. The results of the load forecast are presented in Figure 2. In this figure, it is evident that there are intra-year patterns which are related with the weeks of the year, while the signal is repeated with a specific structure for each week of the year. As can be noticed, the developed model has a very good overall efficiency and pattern capturing capability, since the red curve (Forecasted values) is almost identical to the blue curve (True values). In Figure 2b, the higher degree of detail of the developed network is depicted, at the intra-week patterns, while the separate actual data points at each hour are clearly illustrated. A whole week is presented starting from Sunday and as can be noticed, the weekend days present a lower maximum value compared to the rest of the weekdays. This trend of the load curve is a common feature of power systems of industrialized regions and is explained by the low demand of the industry/commercial sector during these days. On the contrary, the load curves of residential areas do not present this pattern. After the prediction module with the ANN was prepared, the next step was its combination with an optimization algorithm described in the following section.

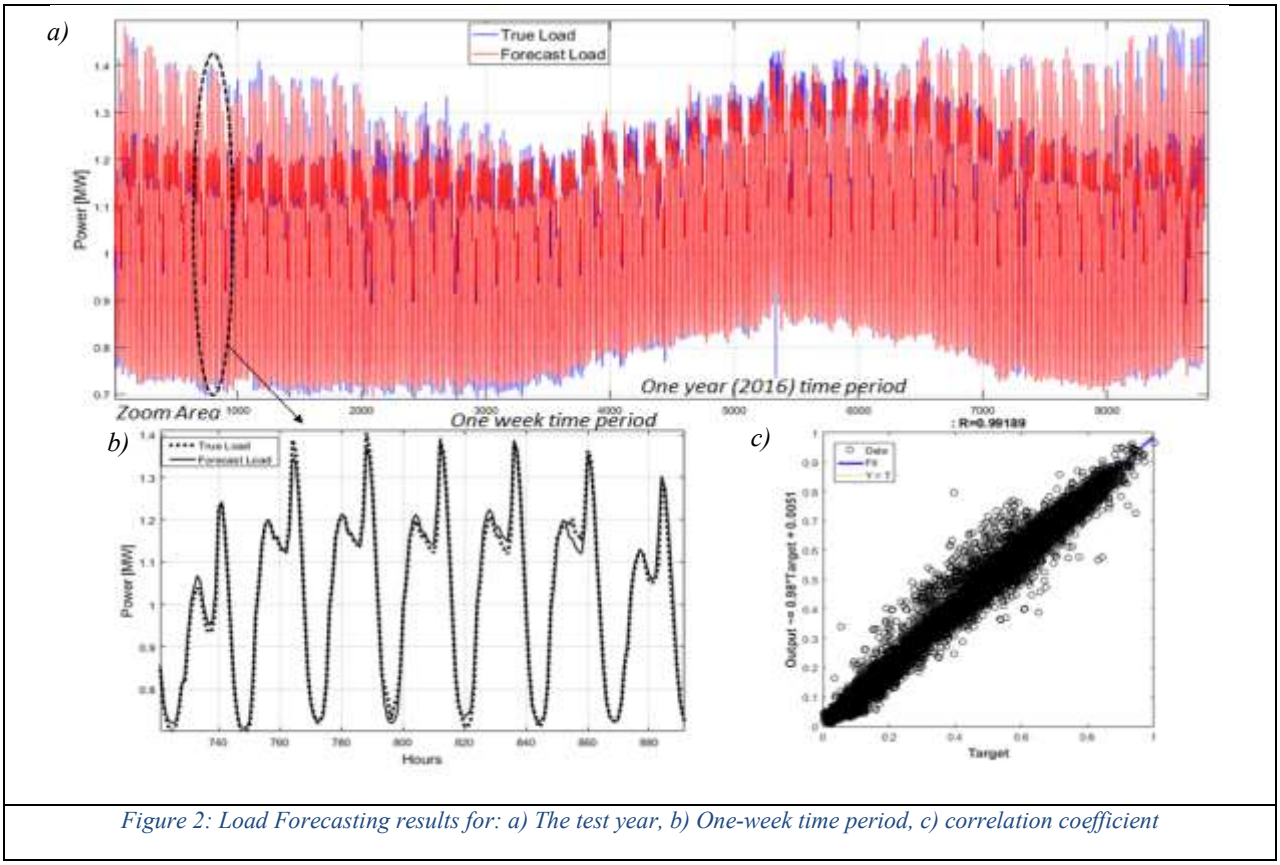

Figure 2: Load Forecasting results for: a) The test year, b) One-week time period, c) correlation coefficient

4. Peak shaving optimization algorithm and power system modelling

In order to take advantage of the load forecasting in the energy management of the island's power system and considering the dominant shape of the load profile (Figure 2), it can be concluded that especially for winter period, the peak values of load are detected during the night hours where the renewable installed PV power is not available.

Regarding the above concern, a BESS capable of storing renewable energy when it is not required and releasing it at night peak demands is a meaningful strategy. However, a BESS should also operate with an optimum plan in order to be sized appropriately and minimize the pay-back period of the investment. In addition, considering that this would be a grid-scaled BESS and that the installed renewable capacity in the island, for the time being, is not enough to cover the load curve at any point, the PV energy storage should be optimized. To this end, an optimization power scheduling algorithm, was developed and deployed for the days that were distinguished based on the clustering method described in the following section.

The under-investigation island's power system has maximum peak demand values of about 1.3-1.5 MWe, which are currently covered by the additional diesel generators that operate at low partial loads, while the installed capacity of PV power is approximately 300 kWe, accounting for around 20% of the peak values. Therefore, in order to achieve zero curtailment and full renewable penetration to the grid, the diesel generators should operate at partial loads under variable conditions during daylight PV production period, while during night they should be capable of a steep and abrupt acceleration to cover the night peak demand. Both of the aforementioned cases contribute to diesel engine efficiency reduction, augmented emissions and high pollutants levels and associated high fuel consumption compared to a steadier operation. A consequence of these is the increase in the electricity production cost.

4.1 Seasonal load profile pattern recognition algorithm/methodology

In order to distinguish and remark the days with a clear night hour peak pattern for applying the developed peak shaving algorithm, a clustering methodology was employed. Towards obtaining high quality clustering results, a dimensionality reduction method was used prior to the clustering algorithm. As a first step of the aforementioned procedure, the data under consideration were pre-processed by employing the z-normalization transformation, which is described by the following formula:

$$x_i' = \frac{x_i - \bar{x}}{\sigma}, where\ i \in N$$ *Equation 7*

, where $\bar{x}$ is the mean value and σ the standard deviation of the original dataset of size N. With the above transformation, the data values were gathered around the x-axis, resulting in a mean value approximately equal to 0 and a standard deviation in the range of 1. As a next step, a data dimensionality reduction technique was used based on the Piecewise Aggregate Approximation (PAA) algorithm, which is commonly used for time series dimensionality reduction [39, 40]. In this way, a smoothing effect of the data shape was achieved, by preserving the most important information and characteristics of the original data but with fewer elements. This algorithm's basic operation is associated with the division of the original time-series data into M equally sized frames and the calculation of the mean values for each frame (*M=9 in this study*). Subsequently, the Symbolic Aggregate approximation (SAX) algorithm was employed, in order to reduce the precision of the time series data values [41]. SAX algorithm is capable of transforming a time-series X of length n into a string of arbitrary length ω, where $\ll n$, typically using an alphabet set (size*(A) = 16 in this study)*. Algorithm's main task is to reduce size of the available data by preserving the most important information (features). The PAA algorithm achieves that by reducing the size of the x-dimension, whereas the SAX algorithm does so by reducing the precision of the y-dimension of the 2-dimensional dataset (x,y). Thus, by combining these two methodologies in the current study, it became feasible to abstract as much information as needed, in order to get satisfactory data clustering results in the following step.

After the above procedure, the pre-processed data were in a suitable form to be imported into the clustering algorithm. Among the various machine learning approaches, the Hierarchical Agglomerative Clustering (HAC) was chosen, because of its simplicity and robustness [42]. Hierarchical clustering is an algorithmic procedure, based on which the data points are successively grouped in nested clusters by merging the nearest of them as identified by the use of an appropriate metric (a measure of distance between the objects). The overall hierarchical structure at the last update of the algorithm is represented as a tree plot (dendrogram). The root of the tree is the unique cluster that gathers all the samples, while the leaves are the clusters with only one sample (each data point), as depicted in Figure 3. In this study, the Euclidean distance was used as metric, which is described for two data points (a, b) by the following equation:

$$\|a - b\|_2 = \sqrt{\sum_i (a_i - b_i)^2}$$ *Equation 8*

As for the linkage criterion, which is used as an indicator for determining the distance of adjacent clusters and whether they should be merged together or not, the minimum variance criterion, also known as Ward's criterion, was employed. Based on Ward's method [43], the observations that are grouped together should result in a reduction of the sum of squared distances of each observation from the average observation in a single cluster. Thus, for two clusters, A and B, a merging action would lead to the merging cost Δ described as:

$$\Delta(A, B) = \frac{n_A n_B}{n_A + n_B} \|\vec{m}_A - \vec{m}_B\|_2^2$$ *Equation 9*

, where $\vec{m}_i$ is the center of cluster i, and n_i is the number of its internal points.

The input to the clustering model employed was the dataset of the 3 years load data (2014, 2015, 2016-test year), after they were processed with the PAA and SAX algorithms. The output of the hierarchical clustering consisted of an array of binaries, which represented the 2 main patterns (1: clear night peak, 0: no clear night peak) for the test year (forecasted from ANN), as they are depicted in Figure 3. This figure presents: a) the load plot of the whole test year for every day and hour, b) the resulting clustering dendrogram, c) the decision table as it was calculated from the clustering algorithm, and d) the general pattern of the derived clusters for indicative days. The two clusters depicted have indeed different overall shape and are clearly distinguished based on the pattern of the encircled areas.

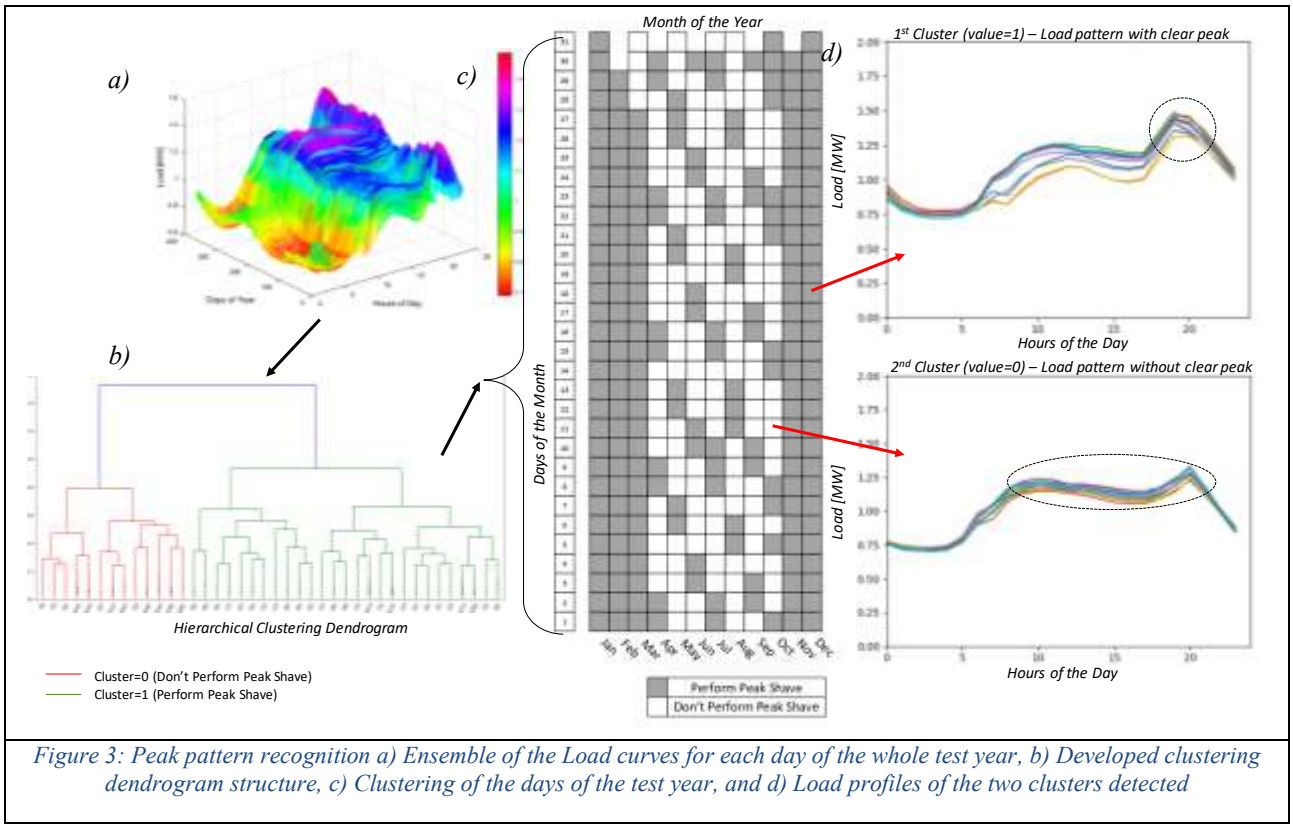

Figure 3: Peak pattern recognition a) Ensemble of the Load curves for each day of the whole test year, b) Developed clustering dendrogram structure, c) Clustering of the days of the test year, and d) Load profiles of the two clusters detected

4.2 Predictive peak shaving methodology

4.2.1 Synthetic Power Curve Formation

Regarding the dominant patterns identified in the section above, a BESS capable of storing renewable energy when it is not required and releasing it at night peak demands is a meaningful strategy. However, a BESS should operate with an optimum plan in order to be appropriately integrated into the system and minimize the pay-back period of the investment. In addition, considering that this would be a grid-scaled BESS and that the installed renewable capacity in the island, for the time being, is not high enough to cover the load curve at any point, the PV energy storage should be optimized. At this point it should be noted that for the shake of a better explanation of the overall procedure, it was considered that the PV production curve is already given for the whole year at an hourly basis (i.e. it was used as an input for the a) self-training, b) testing, and c) evaluation of the algorithm). More details about the PV power curve production and the way it was generated can be found in the next chapter where the system modelling is described.

The first step of the algorithmic procedure was to determine the inputs. These were decided to be the 24 variables vector which contained the demand values of the next day as predicted from the ANN model and the 24 variables vector containing the hourly values of the total PV energy production of the corresponding day. Then the peak reduction level was set to be at 0.1 MW less than the maximum demand value of each day, which roughly represents a 10% of the average daily peak demand. This

value was determined based on the load curve data observation and was evaluated from the values of the peak region relatively to the mid-day load values. However, this parameter could be subjected to optimization in an upgraded version of the algorithm and, in this way, could be matched for each day individually, instead of taking an average constant value. After the peak reduction level or peak shaving level was determined based on the load forecasting of the next day, the area to be removed after the peak reduction was calculated. This is better visualized in Figure 4, where the load curve of the next day is depicted with the solid line, whereas the peak reduction level that is decided to be implemented is represented with the dashed line. This line should cross the load curve at two separate points and in this way a closed area is shaped. This region, which is basically the area under the load curve subtracting the area under the dashed line and is depicted as the grey region in Figure 4, corresponds to the total energy that will be shaved after the algorithm implementation and the generation of the new diesel engines setpoints. It is also clear from the units of the two axes of Figure 4 that the aforementioned area represents the energy values based on the following definition:

$$E_{1\to 2}[MWh] = \int_{t_1}^{t_2} P(t)dt \qquad \textit{Equation 10}$$

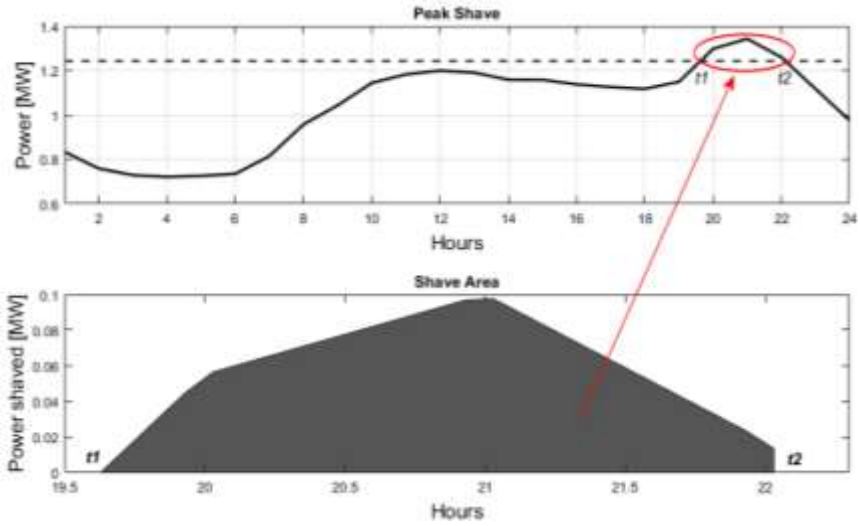

Figure 4: Peak reduction level and the corresponding area between t1 and t2

With the above input parameters defined, the next step was the creation of the combined curve. In order to achieve that, the "offset" value concept was necessary to be utilized. The offset value was defined as a constant load value, which at the first step of the algorithm was initially set equal to the base load value, defined as the minimum of the daily load curve. This offset value was used for the initial combined curve generation, which was subsequently updated during the iterations of the algorithm. The combined curve was defined as either i) the sum of the load curve and the PV power curve, for the load values that were smaller than the offset value, or ii) as the sum of the PV power curve and the offset value, for the load values that were greater than the offset value. This is also mathematically described as below:

$$P_{combined}[MW] = \begin{cases} P_{PV} + P_{load}, & for\ P_{load} < P_{offset} \\ P_{PV} + P_{offset}, & for\ P_{load} \geq P_{offset} \end{cases} \qquad \textit{Equation 11}$$

4.2.2. The "elevator" concept

After the initialization of the algorithm parameters and providing the input values described in the previous section, the next step was the implementation of the "elevator" concept. This was basically the core process of the algorithm according to which the desired effects could be obtained.

Initially, as stated earlier, the offset value was considered as the base load, which was the minimum of the daily load. The PV production curve was then superimposed to this offset level and in this way the offset value was used as a carrier for the total PV power generation curve. The offset level was constantly increasing by a constant step value which was set equal to *dP=1 kW*. This process

was repeated until sufficient surplus area was created. The surplus area was defined as the amount of energy that was overproduced compared to the demand of the corresponding time period. The procedure of updating the offset value is depicted in Figure 5. In this way, the offset level acted as an "elevator" for the PV production curve and at the same time as an upper limit for the diesel engine operation during the off-peak hours.

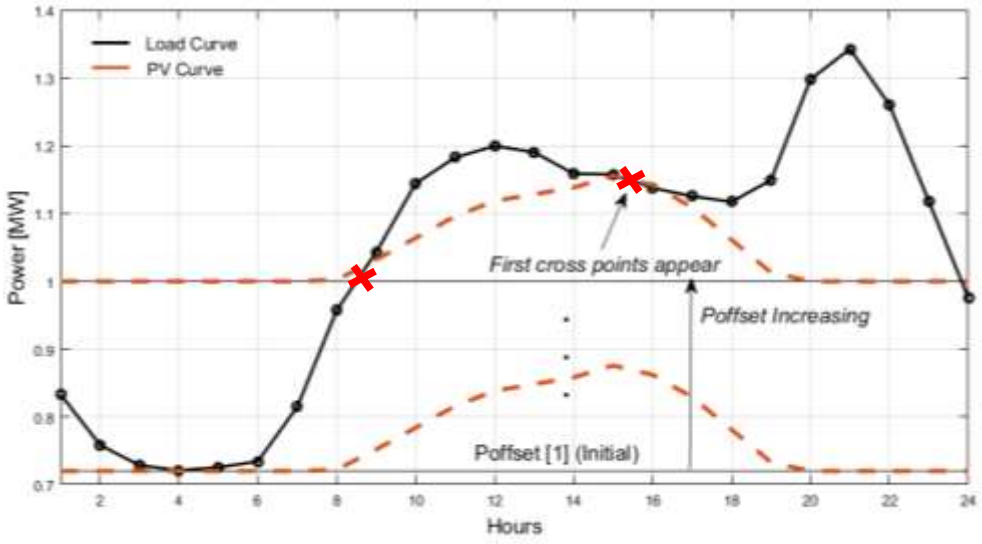

Figure 5: The elevator concept with the corresponding cross points

In the figure above, the process of updating the offset value is described. Initially, the first offset value $P_{offset}[1]$ is set equal to the minimum of the daily load curve. Then, the PV power production curve (dashed line), is superimposed to this line and after each update it is transferred upwards, until the occurrence of the first two cross points (red *cross points x, depicted in Figure 5)* between the elevated PV curve and the load one during the sunlight time period. This condition was needed to be satisfied, since if the curves were intersected before then it would be impossible to "generate" an artificial surplus, because the offset would still be very low. Subsequently, the updates were continued and the final cross points are depicted in Figure 6. These cross points define three separate areas (E_1, E_2, E_3) as can be observed. The two areas are defined from the cross points I - II and II - III correspondingly, while the third area from the cross points III - IV. The first (*points I-II*) and the third *(points III - IV*) areas, define a region in which the combined curve resulting from the updates of the offset is greater than the total demand and therefore the BESS should be able to store the additional energy (i.e. E_1, $E_3 > 0$). For the second area (*points II-III*), the inverse is happening, meaning that the instantaneous produced energy is lower than the load curve and consequently the BESS should provide an additional amount of energy (i.e. $E_2 < 0$). Each update of the offset level, resulted in a new artificially created surplus area, which was calculated as the algebraic sum of the derived orange areas $(E_1 + E_2 + E_3)$. If the total algebraic sum remains negative $(E_1 + E_2 + E_3 < 0)$, meaning that not sufficient surplus energy would be formed, the offset level should keep updating. After each update, the aim of the developed algorithm was to converge to the targeted value, i.e. $E_1 + E_2 + E_3 \rightarrow E_{peak}$, satisfying the termination criterion of the algorithm which can be represented as $E_1 + E_2 + E_3 \approx E_{peak}$, within an acceptable convergence limit range. At this point, it should be clarified that concerning the region formed from the points I to III, in case that the BESS cannot provide the necessary power, then the diesel generator should violate the upper limit rule defined by the offset value in order to maintain the balance of the system. The process described above should be repeated until the last P_{offset} value was reached. This would mean that the net energy (energy to be stored to the BESS minus the energy to be provided by it) should be at least equal to the total energy that would be needed later for the peak shaving to be applied (green area).

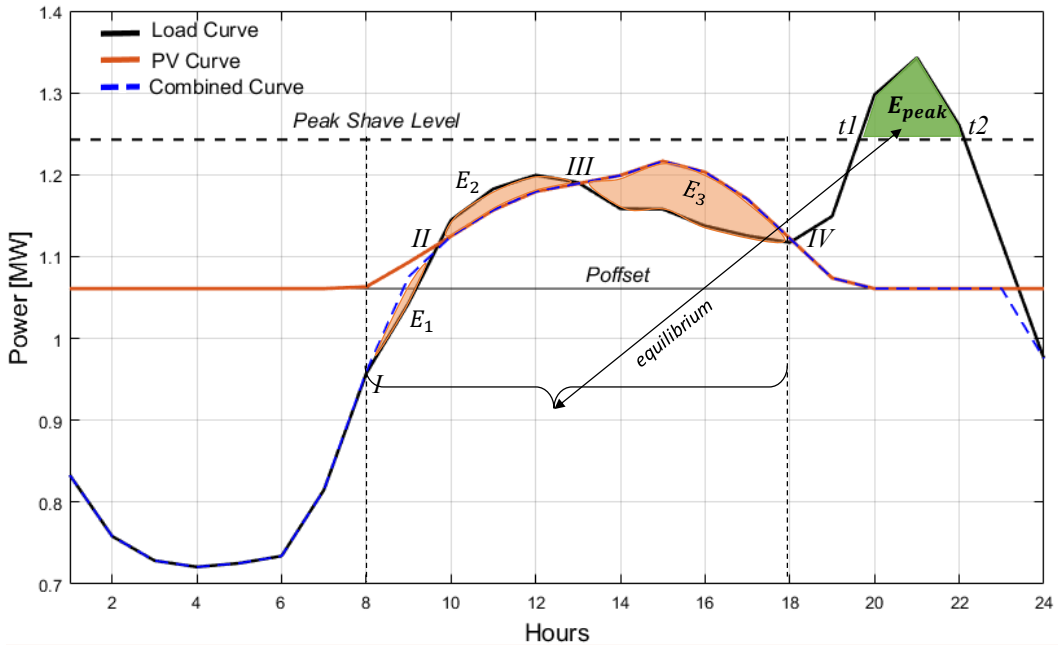

Figure 6: The equivalent areas generated by the "elevator" technique and the equilibrium pursuit

The aforementioned statement could be expressed mathematically as:

$$\int_{t_I}^{t_{IV}} (P_{combined} - P_{load})\, dt \geq \int_{t_1}^{t_2} P_{load}\, dt \qquad \textit{Equation 11}$$

, where t_I and t_{IV} the cross points depicted in Figure 6, and *t1* and *t2* the cross points defined by the peak shaving level, depicted in Figure 4. In order to calculate the above areas as accurately as possible, a linear interpolation was considered between the hourly values of demand and production, which in general is quite close to the actual case.

The overall combined methodology proposed in this study (combining a load forecasting module, a daily load pattern recognition module and the custom power flow scheduling technique) is depicted in Figure 7.

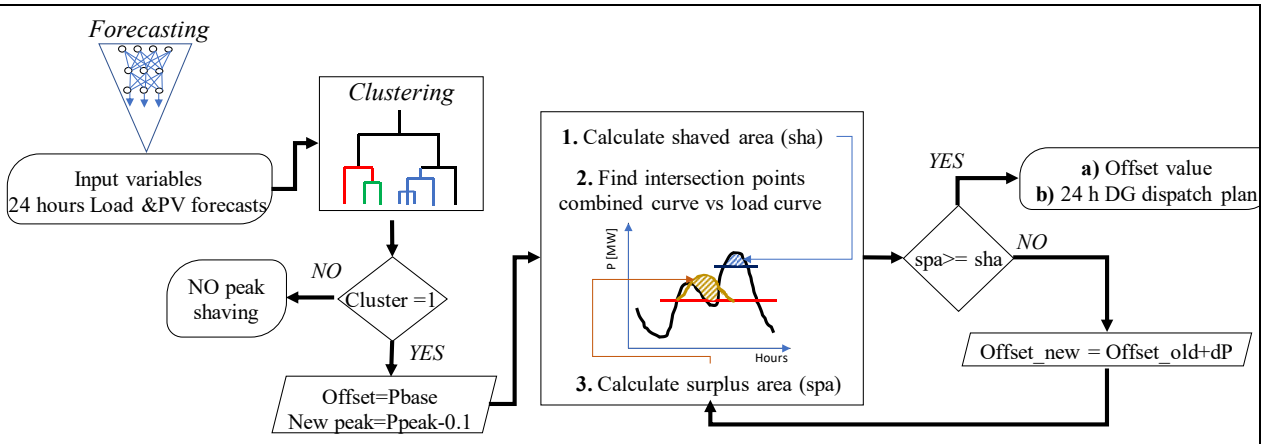

Figure 7: Overall developed methodology flowchart

4.3. APROS BESS model with EMS implementation

The power system's balance is modelled as the aggregation of the signal flows coming from the various energy system components, representing the individual power flows that have to be in an equilibrium so that the balance of the system is preserved. This can be mathematically formulated with the following expression:

$$\left| P_{residual}(t) = \sum_{i=1}^{N_p} P_{inflow,i}(t) - \sum_{i=1}^{N_c} P_{outflow,i}(t) \right| \leq \varepsilon \quad \text{Equation 12}$$

where $N_p = 3$ stands for the different possible energy injections to the grid from each energy production (or storage discharging) system (i.e. the diesel engines, the PV system and the BESS), while $N_c = 2$ stands for the different possible energy sinks (i.e. the system's load and the energy being stored to the BESS). In the above equation, a relaxation variable ε is also used for the system balance, representing the perturbations in the balance of the system which are associated with control actions and deviations in a very small time-scale compared to the hourly-based analysis implemented for the power system simulation. The balance of the system should be preserved at each time step of the simulation and in case this is not possible with the current configuration, the BESS should compensate for restoring the balance, and if even this is not feasible, then the diesel engines should be operated appropriately.

4.3.1 Battery modelling

Initially, the next day forecasted load curve and the PV production are used as an input into the algorithm. The energy production of the installed PV plants is predicted using a validated simulation engine developed by Pfenninger et al. [44] and through which it is possible to yield an hourly based production dependent on the irradiance intensity on the island. As the purpose of this work is the evaluation of the performance of the neural network load forecasting module combined with the energy management of a BESS for peak shaving, the produced renewable energy is considered as a perfect forecast.

Thereafter, the predictive peak shaving algorithm described in previous sections was incorporated in the BESS energy management system, which was modelled in APROS software and simulated for the whole year. An APROS validated multi-cell Lithium battery module was employed in order to model the BESS. The basic equations [45] related to the Lithium battery model are the following:

$$U(t) = V_{OC}(t) \cdot n - \frac{n}{m}\left(R_{series} + R_{cycle} + R_{tr_{sh}} + R_{tr\_ln}\right) \cdot I_{bat}(t) + n \cdot \Delta E(T) \quad \text{Equation 13}$$

In the above equation, $V_{OC}(t)$ represents the open circuit voltage of each cell, which is a function of the remaining capacity and is set at maximum capacity of about 4 V; $I_{bat}(t)$ is the battery current, n =199 and m =169 are the number of cells in series and in parallel respectively; and R_{series} is responsible for the instantaneous voltage drop in battery terminal voltage $U(t)$. The other component of series resistor, R_{cycle}, is used to explain the increase in the battery resistance with cycling. The components R_{tr_sh} and R_{tr_ln} of the battery RC network are responsible for short- and long-time transients in battery internal impedance respectively [46]. Regarding the open circuit voltage and the resistance of the battery's network model, the state of charge of the battery (SOC) needs to be calculated. The battery SOC can be expressed based on the capacity updates as:

$$C(t) = C(t - \Delta t) - I_{bat}(t) \cdot \frac{\Delta t}{3600} \quad \text{Equation 14}$$

$$SOC = SOC_{init} - \int \left(\frac{I_{bat}}{C_{usable}}\right) dt \quad \text{Equation 15}$$

$C(t)$ is the current battery capacity, which is updated at each simulation step Δt. The latter is set equal to $0.2s$, in order to capture small scale dynamic transient phenomena in voltage $U(t)$ and current $I_{bat}(t)$ parameters. The capacity of the battery was limited between the values 0 and the maximum capacity. The initial capacity value is set equal to 50%. This fact is in line with the current trends of the batteries industry, which is constantly upgrading the materials, the structure and the quality of the produced batteries. Such updates and advancements result in an overall efficiency upgrade and allows for the development of deep charge/discharge batteries, maximizing its useful capacity and consequently the capabilities of a BESS. In order to better simulate the degradation of the battery's material and its

ability for energy storage, a capacity fading model was integrated into the battery model of this study. Capacity fading refers to the irreversible loss in the usable capacity of a battery due to time, temperature and cycle number. Generally, a battery is considered to be usable until reaching down to the 80% of its initial capacity [47, 48]. So, modeling the capacity fading is important for predicting the remaining life of the battery. The irreversible usable capacity loss, causing capacity fading, is associated with degradation of the battery, and the loss occurs whether the battery is inactive (so-called "calendar life" losses) or exercised ("cycle life" losses) [49]. Both calendar and cycle life losses of a battery appear to be linear with time and dramatically increase with increasing temperature [48]. Therefore, the effect of temperature must be considered while modeling the capacity fading for a battery. The calendar and cycle life losses lead to a capacity correction factor to determine the remaining usable battery capacity. Thus, the capacity fading was modelled considering the correlation between the battery temperature and capacity. In this way, the maximum capacity of the battery was calculated as a fraction of the nominal capacity considering both calendar and charging losses, based on the following equations:

$$C_{max}(t) = C_{nom} \cdot [1 - (f_{sl}(t) + f_{cl}(t))] \quad \textit{Equation 16}$$

C_{nom} is the nominal capacity of the BESS which is set equal to 2000 Ah. $C_{max}(t)$ is the maximum remaining capacity of the battery, which is affected by battery aging and degradation effects, through coefficients f_{sl} and f_{cl} that represent the lifetime storage loss fraction and the lifetime cycle loss fraction respectivelyThe SOC calculation at each time step was based on the corresponding maximum battery capacity as resulted by taking into account the degradation effect. The storage losses and the cycle losses can be expressed as

$$f_{sl} = \int sl_1 \cdot e^{\frac{sl_2}{RT}} \cdot \frac{dt}{100 \cdot 2592000} \quad \textit{Equation 17}$$

$$f_{cl}(t) = f_{cl}(t - \Delta t) + \left[N_{eqv}(t) + k_2 \left(N_{eqv}(t) - N_{eqv}(t - \Delta t)\right)\right] \quad \textit{Equation 18}$$

, where the number of full cycles and the losses per cycle can be then represented according to the following equations respectively:

$$N_{eqv} = \int \frac{\frac{1}{2}|I_{bat}|}{3600 \cdot C_{max}} \quad \textit{Equation 19}$$

$$\frac{\partial SOC_{cycle}}{\partial N_{eqv}} = k_1 N_{eqv} + k_2 \overset{\frac{\partial}{\partial t}}{\Rightarrow} \frac{\partial SOC_{cycle}}{\partial t} = (k_1 N_{eqv} + k_2)\frac{\partial N_{eqv}}{\partial t} \quad \textit{Equation 20}$$

The coefficients k_1, k_2, k_3 in the above equations depend on the temperature of the battery and further details can be found in [50].

4.3.2 Control configuration for the BESS

For the implementation of a complete simulation framework based on forecasting capability, as proposed in this study, a top to bottom approach should be followed for the development of the management algorithm responsible for controlling the power system operation. The planned energy systems setpoint information was directly related with the operation of the battery, which should track a planned power delivery trajectory, derived from the developed algorithm described in section 4.2.

From the above it is evident that the operation of the BESS was predefined based on the prediction module and the algorithm. However, the planned trajectory cannot be reproduced in the real dynamic operation of the power system for the following reasons. At first, the power system's demand values were slightly different from the forecasted demand values which can be attributed to the neural network errors. Despite the overall good quality of the network prediction, which resulted in a satisfactory mean absolute percentage error (MAPE=1.715%) for the year of the simulation (2016),

when focusing on specific load values, the error can be higher relatively to the overall system performance. Thus, during the dynamic simulation of the power system with a fine time resolution, the instantaneous errors of the forecasting module may result in significant deviations from the expected values and consequently the balance of the system could be risked. Another source of error regarding the dynamic simulation of the power system with the integration of the supervisory algorithm originated from the current state of the battery system. Since the detailed BESS model described in the previous section (4.3.1) was not considered by the algorithm that generated the setpoint values, it was not possible to estimate the different actual states of the battery during the setpoint calculation. The variables that have the most direct and significant impact on the state of the battery are the current capacity *C*, the state of charge (SOC) and the maximum possible current injection. The last limitation originates from the maximum possible power delivery from the battery. Another important factor that could not be estimated before the dynamic simulation was the aging impact and the degradation of the battery's maximum capacity.

For the reasons described above, it is clear that in order to preserve the system balance and to track in the best possible way the predefined system operation, a real time control system should be employed. This serves mainly to monitor the system for sudden changes and consider the appropriate actions to be made for restoring the balance.

In Figure 8, a schematic representation of the real time charge / discharge controller of the BESS, adopted in this study, is presented. As can be noticed, a cascade configuration was introduced, which was based on simpler proportional-integral single input single output controllers. This setup was adopted mainly because of its simplicity in structure and the commonly available PI controllers in industry. From Figure 8 it is possible to observe that there are two different controllers, i.e. one for the charging process control and another for the discharge process control. Both of them acquire their setpoints to fit on the output of a centralized controller, which is responsible for regulating the system residual. The power system residual can be found in Equation 12 and is basically an indicator of the excess or shortage of energy in the power system. Thus, the setpoint of this controller was set equal to zero (0) so that the error is regulated and the balance of the system is preserved.

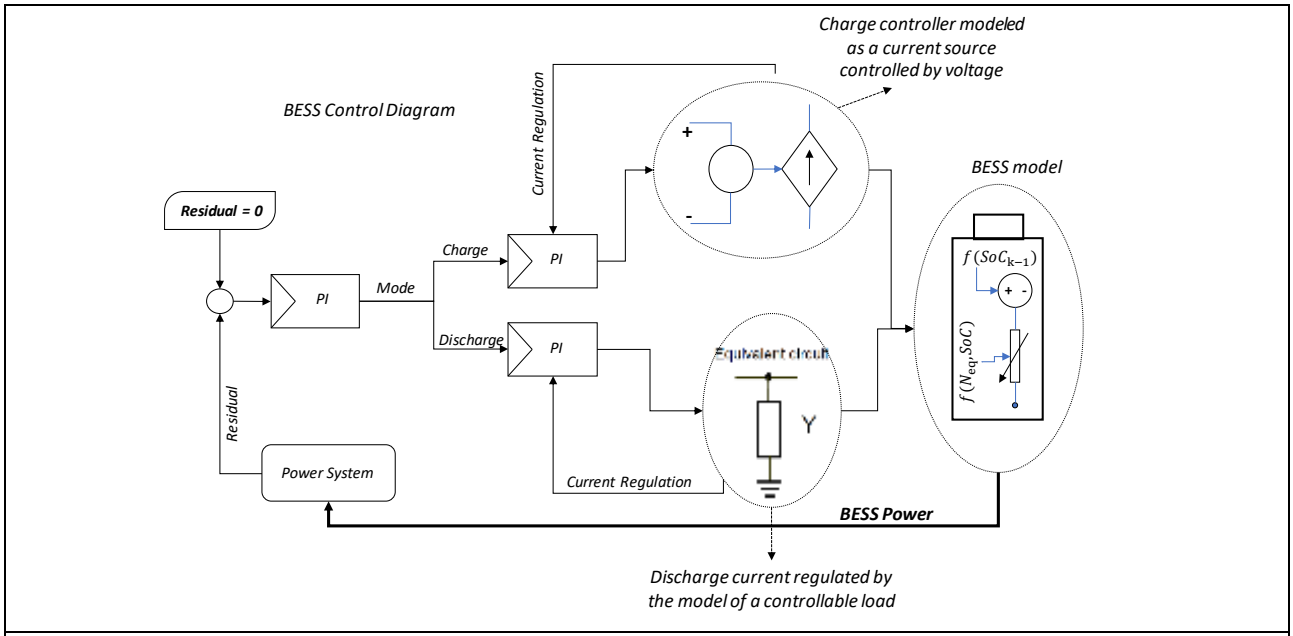

Figure 8: BESS control system configuration

Then, the central controller fed its output to the other controllers, which were devoted to the current regulation of the battery. Specifically, the discharge process was modeled with a controllable load. In this way, the discharge current injected from the battery to the grid was regulated by changing the value of the internal resistance of the controllable load and, consequently, the appropriate amount of power was injected into the grid. Regarding the charging mode, the power being stored inside the battery was controlled by regulating the charging current with the help of a voltage controlled current

source as depicted in Figure 8. In this way, a DC controllable source model was used for the current regulation task during charging.

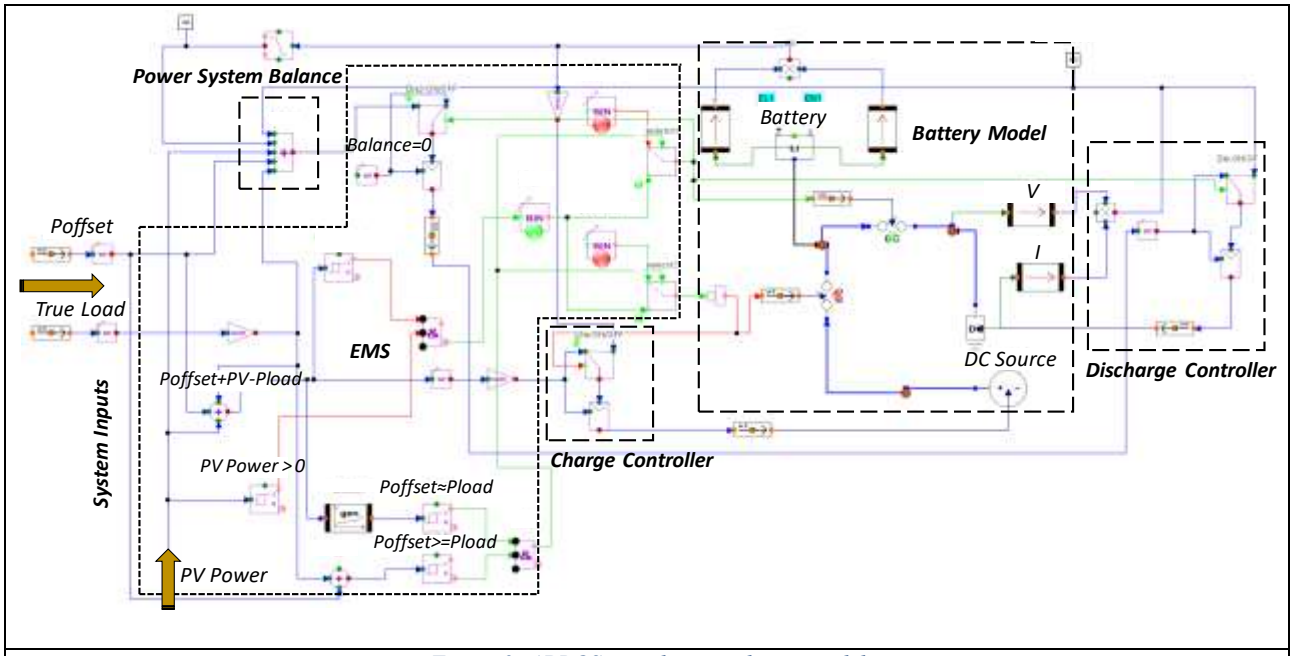

Figure 9: APROS complete simulation model

Combining the signal and electrical modules described above, it was possible to develop the whole system model in APROS software platform. It was also possible to model the energy management system that supervised the system operation, based on the previously developed strategy and relatively simple logic controllers. In Figure 9, the complete APROS model is depicted. From this picture it is possible to observe the following basic subsystems: a) the system inputs, b) the power system balance, c) the battery model, d) the charge and discharge controllers, and finally e) the EMS. The balance of the system was modeled as a signal adder that was responsible for the summation of all the incoming signals which represented power flows. The result, which was named as "residual", was considered as an output signal and was then fed to the balance of system controller. The BESS was modelled based on the Lithium battery module with the corresponding set of equations described in 4.3.1. The system inputs to the model are the 24-hour diesel generators set points for every day of the year which are calculated according to the methodology described in the previous section, the real demand curve of the island for 2016 and the perfect PV forecasted power values for the same year. As shown in Figure 9, the EMS that controls the system is formulated as a binary signal logic, which is responsible for the operation state of the BESS. In particular, when PV power is available at daylight and at the same time the sum of the diesel generators' offset set-point and the PV power is greater than the current load demand, the EMS commands a charging state for the battery. If PV power is not available or the aforementioned sum is less than the load demand, the battery should discharge as much energy as needed. In case either the offset set-point of the diesel generators is greater than the actual load demand or the absolute value of the residual (defined as the diesel power plus the PV power minus the load demand) is smaller than 0.1 kW, then the BESS should be in idling mode and ready for a future incident. Thanks to this operation plan, not only BESS is charged with renewable energy that can be used at a future time, but also the false scheduling due to forecasting errors is compensated at the same time.

5. Results of the dynamic simulations

After the system model configuration was completed, the power system yearly operation was simulated according to the rules and the operational strategies mentioned above. Thus, it was possible to estimate the performance of the predictive EMS algorithm regarding the impact of load forecasting to the real time operation of the BESS.

As described in the previous section, the system power balance was used as a criterion for power generation-consumption balancing and it was being monitored, in order to be constantly zero (i.e. no over/under production was allowed). For that reason, the battery power delivered to the system was controlled according to this specification. However, at specific times over the year period, the power balance was not achieved due to individual large forecast errors or operational limitations owed to the state of charge of the battery. This surplus or deficit of energy was considered to be compensated by the diesel engines, supposing a flexible operation with small deviations around their base scheduled operating point, as forecasted. A good overall performance of the system was obtained with a significant success in smoothening the load curve around the engines predicted operating points. As seen in Figure 10, the new achieved operation of the diesel engines consisted of basically two levels, i.e. one related with the offset derived from the optimization algorithm and one owed to successful peak shaving implementation. In this figure, the simulation results are presented for a one-week duration, enabling the comparison of two different operational strategies of the diesel engines. The first approach named as "OLD Diesel" corresponds to the diesel engine operation if the system could absorb all possible PV energy production, meaning zero curtailment, despite the lack of load forecasting. The second approach named as "NEW Diesel" corresponds to the proposed methodology. Based on Figure 10, it is clear that the "NEW Diesel" operation is much smoother than the OLD one, while the produced PV energy is completely absorbed by the system, by supplying during the time periods of peak shaving the artificially achieved excess PV power during the prior off-peak periods. This ensures that all renewable energy produced is supplied to the grid resulting in a predicted and planned zero curtailment.

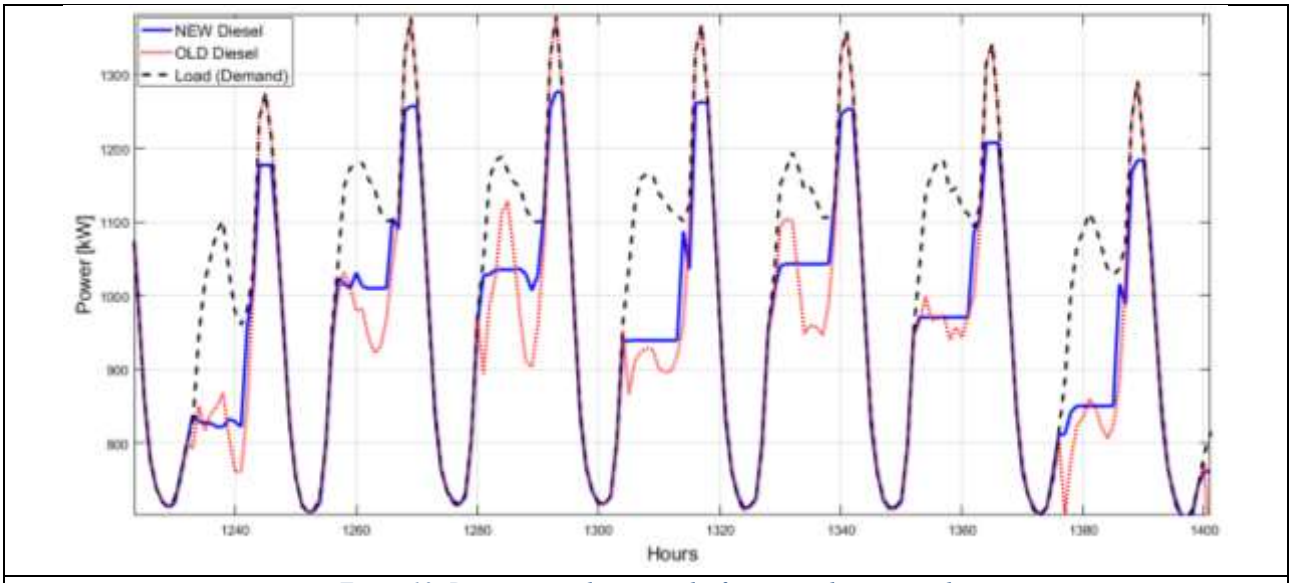

Figure 10: Dynamic simulation results for a typical winter week

Figure 11 depicts the calculated results during a single day operation of the week presented in Figure 10. As seen, with the proposed methodology the diesel engines operate in a more monotonic mode, owed to the calculated offset level and it is possible to avoid in a great extent the valleys and crests due to the PV generation at the specified time-periods. These time varying and unplanned operating conditions are mitigated with the proposed BESS operation, leading to a significant improvement in the magnitude and the gradient of the engine's ramp-up for the following peak event. In this way, a more precise dispatch planning of the diesel engines can be yielded and the allocation of fewer additional engines to cover the ramp-up of the load curve can be achieved. In addition, the acceleration rate of the engines, depicted through the gradient of their operation in Figure 11, is decreased. Given the direct relation of this gradient and fuel consumption, decreasing this gradient results in a smoother, less fuel consuming and more cost-effective engine operation.

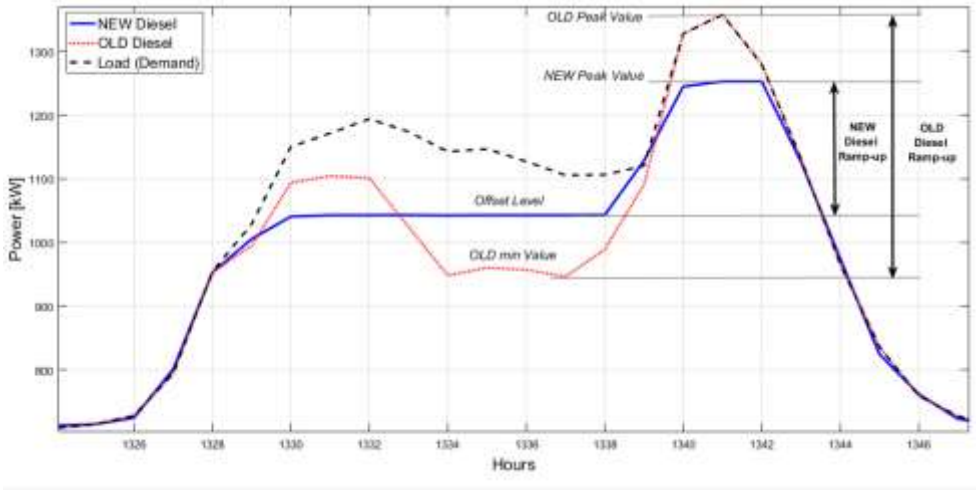

Figure 11: Dynamic simulation results for a single day operation

The aforementioned effects on the operation of the system are also depicted from the BESS side in Figure 12, where the correlation of the BESS delivered power, state of charge and PV production are presented. It is revealed that during the time period of PV production, the BESS stores energy that is going to be supplied later on during the peak demand. For that reason, the SOC of the BESS ranges around its daily maximum values right before the peak demand event and subsequently it supplies the daily maximum power when the peak demand event is reached. The maximum PV energy production is followed by the maximum value of the battery's SOC, which in turn is followed by the maximum value of the power delivered from the BESS. The latter, also coincides with the maximum peak demand value, which is another indication that the peak demand is satisfied from the stored renewable energy.

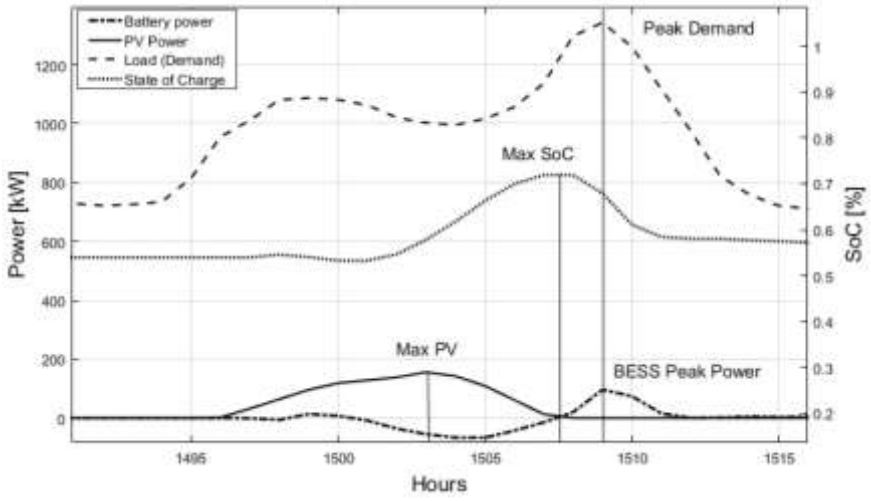

Figure 12: Single day operation BESS results

In order to assess the ability of the developed algorithm (section 4) to predict a reasonable behavior of the battery system, the scheduled and the resulted battery power trajectories were compared. In Figure 13, the injected and absorbed power flows from and to the battery system respectively are presented. The injected power is regarded as a positive battery power value while the absorbed energy, associated with storage, is represented by the negative battery power values. Specifically, in Figure 13, the two aforementioned trajectories are plotted on the same diagram for a random day of the year (day 63), which corresponds to a typical winter day. The red dashed line represents the scheduled trajectory of the battery, which is predicted based on the load forecasting of the next day and the algorithmic procedure for storing enough energy to cover the peak load area in a later time period. The black solid line corresponds to the real battery usage after the system was simulated with the real time control and the energy management systems integrated. It can be observed that the scheduled battery profile is similar to the actual one that was monitored during the system dynamic

simulation. In particular, the two profiles present the same patterns and trends regarding the time periods of battery system charging and discharging, while a delay in the actual case compared to the scheduled one can be noticed. This can be attributed to the real time dynamics of the system which are mainly affected by two major aspects. The first one is related to the current battery status, concerning the variable operational limits and gradients and the response time of the battery's dynamic behavior. The second aspect is related to the true demand values that are faced by the battery system. These values can be slightly different from the forecasted ones, based on which the battery operation was planned. However, the overall battery behavior seems to follow the mainstream daily profile which is characterized from storing the artificially generated excess of renewable energy during the sunlight time periods and injecting it back to the grid during the peak demand time periods. Furthermore, the actual injected power observed in Figure 13 is very close to the scheduled power injection value, which was estimated as the peak reduction level in section 4.2.1, equal to 0.1 MW of the daily maximum power demand, as the last one was predicted by the neural network.

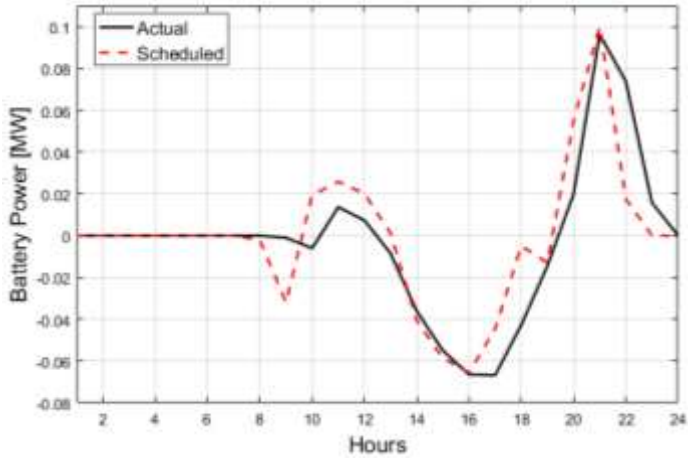

Figure 13: Battery actual vs scheduled power flows for day 63

6. Conclusions

In the present study, a predictive EMS based on load forecasting was introduced and integrated with the operation of a BESS for peak demand reduction with renewable energy, for a South-European islanded power system with relatively higher load consumption compared to its RES production. The results of the sophisticated synergy of prediction, classification and a newly developed algorithm with real time control of the BESS, revealed that peak shaving with renewable energy, load levelling and smoothing in conjunction with a better diesel generators scheduling can be achieved, especially for larger power systems for which the renewable penetration is constantly increasing to approach the consumption level but has not yet exceeded it.

The results obtained with the developed artificial neural network (ANN) model were satisfying, despite the simplicity of its structure and the number of input variables. The forecasting quality of the network was estimated with the calculation of a commonly used index (metric) in machine learning algorithms, called mean absolute percentage error (MAPE=1.715%). The training of the developed neural network module was based on the hourly demand values for two consecutive year time periods (2014, 2015) and the model was able to predict the daily load curve of the next day, on an hourly basis, for the test year (2016). Then, with the development of the clustering module, it was possible to identify the suitability of the day ahead night hour load pattern for peak shaving and smoothing which was implemented by the algorithm developed in this study.

This custom-made algorithm used as input variables the forecasted load and the PV power generation of the next day, while the peak load reduction level could also be determined. The algorithm's main goal was to manage the energy flows of the power system, in order to counterbalance the high peak demand of the night hours, which was the most common pattern

associated with the island's power curve during the winter time period, as is also the case for other similar power systems. This pattern is primarily related with abrupt load changes and steep gradients of the net load curve, which are formed due to the obvious non time-coincidence of the peak renewable power generation values with the peak demand ones and it is associated with the deterioration of the net load curve as the renewable penetration increases.

The developed algorithm was integrated to the system's dynamic model, which was developed in APROS simulation platform. The dynamic simulation of the system proved the capability of the developed EMS to manage the BESS power flow in order to cover the forthcoming night hour peak demand and also to find an optimum operating level of the diesel generators. This resulted in a steady and smooth operation, without abrupt load changes and steep gradients.

The system was simulated for a whole year and except from the peak shaving of the load curve by using stored PV energy, a significant reduction of the variability of diesel generators operation was also achieved. The proposed method reinforced the power grid ability to integrate renewable power in a more robust and planned way, leading to zero curtailment and possible cost reduction through fuel savings.

A future step for the improvement of this method could be the battery size optimization and the integration of PV power production forecasting to the scheduling algorithm. Also, the fuel consumption of the diesel generators, incorporated into a techno-economical study, could further enlighten the economic feasibility of the proposed configuration. Furthermore, as a next step a more detailed representation of the power inverter with small time scales control could be considered.

Acknowledgements

This work has been carried out in the framework of the European Union's Horizon 2020 research and innovation programme under grant agreement No 731249 (Smart Islands Energy Systems - SMILE).

Abbreviations

ANN: Artificial Neural Network
BESS: Battery Energy Storage System
DG: Diesel Generator(s)
EMS: Energy Management System
MAE: Mean Absolute Error
MSE: Mean Squared Error
MAPE: Mean Absolute Percentage Error
NWM: Numerical Weather Model
PV: Photovoltaic
SoC: State of Charge

Nomenclature

$\vec{b}$: network neurons biases
C: BESS capacity, Ah
$\vec{e}$: network errors
$f(u)$: neurons activation function
I_{bat}: BESS current, A
J: Jacobian matrix of the network errors
N: BESS charging cycles

P_{PV} : PV produced power, kW

P_{offset} : offset power level for the DG, kW

P_{load} : true demand power of the island's power system, kW

$P_{combined}$: combined curve, kW

$P_{residual}$: residual power, kW

R_i : battery internal resistances, Ohm

R: correlation coefficient

$\vec{t}$: network target values

$\vec{u}$: network inputs

V_{OC} : BESS cell open circuit voltage, V

U: voltage over BESS terminals, V

$\vec{x}_k$: vector of weight and biases at k iteration

$\vec{y}$: network outputs

Greek symbols

μ relaxation coefficient of Levenberg-Marquardt method

Δt simulation time step, s

σ standard deviation

Subscripts and superscripts

eqv: equivalent

max: maximum

nom: nominal

init: initial

References

[1] Das Kumar U., Tey S.K., Seyedmahmoudian M., Mekhilef S., Idris I.Y.M., Van Deventer W., Horan B., Stojcevski A., Forecasting of photovoltaic power generation and model optimization: A review, Renewable and Sustainable Energy Reviews 2018;81:912-928.

[2] California Independent System Operator, "What the duck curve tells us about managing a green grid", http://large.stanford.edu/courses/2015/ph240/burnett2/docs/flexible.pdf

[3] Chua H.K., Lim S.Y., Morris S., A novel fuzzy control algorithm for reducing the peak demands using energy storage system, Energy 2017;122:265-273.

[4] Tsekouras G.J., Kanellos F.D., Kontargyri V.T., Tsirekis C.D., Karanasiou I.S., Elias CH.N., Salis A.D., Kontaxis P.A., Mastorakis N.E., Short term load forecasting in Greek intercontinental power system using ANNs: a study for input variables, Proceedings of the 10th WSEAS International Conference on NEURAL NETWORKS; 2009.

[5] Mordjaoui M., Haddad S., Medoued A., Laouafi A., Electric load forecasting by using dynamic neural network, Int. J. of Hydrogen Energy 2017;42:17655-17663.

[6] Hahn H., Meyer-Nieberg S., Pickl S., Electric load forecasting methods: Tools for decision making, European Journal of Operational Research 2009;199:902-907

[7] Satish B., Swarup K.S., Srinivas S., Rao Hanumantha A., Effect of temperature on short term load forecasting using an integrated ANN, Electric Power Systems Research 2004;72:95-101.

[8] Brodowski S., Bielecki A., Filocha M., A hybrid system for forecasting 24-h power load profile for Polish electric grid, Applied Soft Computing 2017;58:527-539.

[9] Moral-Carcedo J., Perez-Garcia J., Integrating long-term economic scenarios into peak load forecasting: An application to Spain, Energy 2017;140:682-695.

[10] Saviozzi M., Massucco S., Silvestro F., Implementation of advanced functionalities for Distribution Management Systems: Load forecasting and modelling through Artificial Neural Network ensembles, Electric Power Systems Research 2019;167:230-239

[11] Yang A., Li W., Yang X., Short-term electricity load forecasting based on feature selection and Least Squares Support Vector Machines, Knowledge-Based Systems 2019;163:159-173

[12] Abreu T., Amorim J. A., Santos-Junior R.C., Lotufo D.P. A., Minussi R.C., Multinodal load forecasting for distribution systems using a fuzzy-artmap neural network, Applied Soft Computing 2018;71:307-316

[13] Weniger J., Bergner J., Quaschning V., Integration of PV power and load forecasts into the operation of residential PV battery systems, 4th Solar Integration Workshop.

[14] Bottiger M., Paulitschke M., Bocklisch T., Innovative Reactive Energy Management for a Photovoltaic Battery System, Energy procedia 2016;99:341-349.

[15] Angenendt G., Zurmuhlen S., Mir-Montazeri R., Magnor D., Uwe Sauer D., Enhancing Battery Lifetime in PV Battery Home Storage System Using Forecast Based Operating Strategies, Energy Procedia 2016;99:80-88.

[16] Yoo J., Park B., An K., AI-Ammar E.A., Khan Y., Hur K., Kim J.H., Look-Ahead Energy Management of a Grid-Connected Residential PV System with Energy Storage under Time Based Rate Programs, Energies 2012;5:1116-1134.

[17] Sun C., Sun, F., Moura J.S., Nonlinear predictive energy management of residential buildings with photovoltaics & batteries, Journal of Power Sources 2016;325:723-731.

[18] Arcos-Aviles D., Pascual J., Guinjoan F., Marroyo L., Sanchis P., Marietta M.P., Low complexity energy management strategy for grid profile smoothing of a residential grid-connected microgrid using generation and demand forecasting, Applied Energy 2017;205:69-84.

[19] Zhao B., Chen J., Zhang L., Zhang X., Qin R. Lin X., Three representative island microgrids in the East China Sea: Key technologies and experiences, Renweable and Sustainable Energy Reviews 2018;96:262-274

[20] Sepasi S., Reihani E., Howlader A.M., Roose R.L., Matsuura M.M., Very short-term load forecasting of a distribution system with high PV penetration, Renewable Energy 2017;106:142-148.

[21] Reihani E., Ghorbani R., Load commitment of distribution grid with high penetration of photovoltaics (PV) using hybrid series-parallel prediction algorithm and storage, Electric Power Systems Research 2016;131:224-230.

[22] Reihani E. Sepasi S., Roose L.R., Matsuura M., Energy management at the distribution grid using a Battery Energy Storage System (BESS), Electrical Power and Energy systems 2016;77:337-344

[23] Reihani E. Mottaleb M., Ghorbani R., Saoud S.L., Load peak shaving and power smoothing of a distribution grid with high renewable energy penetration, Renewable Energy 2016;86:1372-1379

[24] Halfmann F., Alhaider F., Wendiggensen J., Gerhard S. (2017) A Predictive Control Strategy for Battery Energy Storage Systems to combine Peak Shaving with Primary Frequency Control. In: Schulz D. (eds) NEIS Conference 2016. Springer Vieweg, Wiesbaden

[25] Sossan F., Paolone M., Integration and Operation of Utility-Scale Battery Energy Storage Systems: the EPFL's Experience, IFAC-PapersOnline 2016;49:433-438.

[26] Mazzola S., Vergara C., Astolfi M., Li V., Perez-Arriaga I., Macchi E., Assessing the value of forecast-based dispatch in the operation of off-grid rural microgrids, Renewable Energy 2017;108:116-125.

[27] Syed I.M., Raahemifar K., Predictive energy management and control system for PV system connected to power electric grid with periodic load shedding, Solar Energy 2016;136:278-287.

[28] Syed I.M., Raahemifar K., Energy advancement integrated predictive optimization of photovoltaic assisted battery energy storage system for cost optimization, Electric Power systems Research 2016;140:917-924.

[29] Frédéric Colas, Di Lu, Vladimir Lazarov, Bruno François, Hristiyan Kanchev. Energy management and power planning of a microgrid with a PV-based active generator for Smart Grid Applications. IEEE Transactions on Industrial Electronics, Institute of Electrical and Electronics Engineers, 2011, 58 (10), pp.P. 4583-4592.

[30] Delfino F., Ferro G., Robba M., Rossi M., An architecture for the optimal control of tertiary and secondary levels in small-size islanded microgrids, Electrical Power and Energy Systems 2018;103:75-88

[31] Petreus D., Etz R., Patarau T., Cirstea M., An islanded microgrid energy management controller validated by using hardware-in-the-loop emulators, Electrical Power and Energy Systems 2019;106:346-357

[32] Hu J., Xu Y., Cheng W. K., Guerrero M.J., A model predictive control strategy of PV-Battery microgrid under various power generations and load conditions, Applied Energy 2018;221:195-203

[33] Hu J., Shan Y., Xu Y., Guerrero M.J., A coordinated control of hybrid ac/dc microgrids with PV-wind-battery under variable generation and load conditions, Electrical Power and Energy Systems 2019;104:583-592

[34] Hosseinimehr T., Ghosh A., Shahnia F., Cooperative control of battery energy storage systems in microgrids, Electrical Power and Energy Systems 2017;87:109-120

[35] Garcia-Plaza M., Carrasco Eloy-Garcia J., Alonso-Martinez J., Asensio Pena A., Peak shaving algorithm with dynamic minimum voltage tracking for battery storage systems in microgrid applications, Journal of Energy Storage 2018;20:41-48

[36] El-Bidairi K.S., Hung Duc Ngyuyen, Jayasinghe S.D.G., Mahmoud T.S., A hybrid energy management and battery size for standalone microgrids: A case study for Flinders Island, Australia, Energy Conversion and Management 2018;175:192-212

[37] S. Haykin. Neural Networks: A Comprehensive Foundation. Prentice Hall, 1994

[38] Saha, S., et al. 2011, updated monthly. NCEP Climate Forecast System Version 2 (CFSv2) Selected Hourly Time-Series Products. Research Data Archive at the National Center for Atmospheric Research, Computational and Information Systems Laboratory

[39] Yi B.-K., Faloutsos C., Fast Time Sequence Indexing for Arbitrary Lp Norms, Proceedings of the 26th International Conference on Very Large Data Bases, Cairo, Egypt, 2000

[40] Keogh E.J., Chakrabarti K., Pazzani M.J., Mehrotra S., Dimensionality Reduction for Fast Similarity Search in Large Time Series Databases. Knowledge and Information Systems, vol. 3, pp. 263-286, 2001

[41] Lin J., Keogh E.J., Lonardi S., Chiu B.Y., A symbolic representation of time series, with implications for streaming algorithms, Proceedings of the 8th ACM SIGMOD workshop on Research issues in data mining and knowledge discovery, DMKD 2003, San Diego, California, USA, June 13, 2003

[42] Saxena A., Prasad M., Gupta A., Bharill N., Prakash P. O., Tiwari A., Er M. J., Ding W., Lin C.T. A Review of Clustering Techniques and Developments. Neurocomputing, vol. 267, pp. 664-

681
[43] Joe H. Ward Jr. (1963) Hierarchical Grouping to Optimize an Objective Function, Journal of the American Statistical Association, 58:301
[44] Pfenninger S., Staffell I., Long-term patterns of European PV output using 30 years of validated hourly reanalysis and satellite data, Energy 2016;114:1251-1265.
[45] Komulainen R., Ylijoki J., Direct Current Electrical System of Apros, VTT; 2012.
[46] Erdinc O., Vural B., Uzunoglu M., A dynamic lithium-ion battery model considering the effects of temperature and capacity fading, 2009 International Conference on Clean Electrical Power, ICCEP 2009. 383 - 386. 10.1109/ICCEP.2009.5212025.
[47] B. Kennedy, D. Patterson and S. Camilleri, “Use of lithium-ion batteries in electric vehicles”, Journal of Power Sources, vol. 90, pp. 156–162, 2000.
[48] P. Ramadass, B. Haran, R. White and B. N. Popov, “Mathematical modelling of the capacity fade of Li-ion cells”, Journal of Power Sources, vol. 123, pp. 230–240, 2003.
[49] R. Spotnitz, “Simulation of capacity fade in lithium-ion batteries”, Journal of Power Sources, vol. 113, pp. 72-80, 2003.
[50] Huld T., Gottschalg R., Beyer G. H., Topic M., Mapping the performance of PV modules, effects of module type and data averaging, Solar Energy, 2010;84:324-338